J|A|C|S
ARTICLES
Published on Web 10/15/2004

A Spectroscopic Investigation of Carbon−Carbon Bond Formation by Methylene Insertion on a Ag(111) Surface: Mechanism and Kinetics

Weixin Huang† and John M. White*

Contribution from the Department of Chemistry and Biochemistry, Center for Materials Chemistry, The University of Texas at Austin, Austin, Texas 78712

Received May 3, 2004; E-mail: jmwhite@mail.utexas.edu

Abstract: Using reflection−absorption infrared spectroscopy (RAIRS) and temperature-programmed reaction spectroscopy (TPRS), we have investigated the cross-coupling reaction between CH_2(a) and CF_3(a) on a Ag(111) surface. CH_2(a) and CF_3(a) are generated by thermal decomposition of adsorbed CH_2I_2 and CF_3I. RAIRS results unambiguously demonstrate that CH_2(a) inserts into the Ag−CF_3 bond to produce adsorbed CF_3CH_2(a), which upon heating selectively undergoes β-fluorine elimination to form $CH_2{=}CF_2$. Increasing the CH_2(a) and CF_3(a) coverage leads to the sequential insertion of CH_2(a) into Ag−CF_3, as evidenced by $CH_2CH_2CF_3$(a) formation detected with RAIRS. Prior to the insertion reaction, the evidence favors islanding of fragments. The methylene insertion reaction is so facile that it occurs at cryogenic temperatures (120 K). Time-resolved RAIRS (TR-RAIRS) results at selected temperatures reveal an activation energy of 5.8 kJ/mol. Our results provide, for the first time, direct spectroscopic information about the mechanism and kinetics of the methylene insertion reaction.

1. Introduction

Fischer−Tropsch synthesis over transition metals is one of the most important heterogeneous catalytic reactions.[1] The key feature of this reaction is the formation of carbon−carbon bonds and the production of higher hydrocarbons from carbon monoxide and hydrogen. Numerous researchers, using thermal, photochemical, or electron-impact dissociation of alkyl halides under ultrahigh vacuum (UHV) conditions, have generated alkyl groups on single-crystal metal surfaces to study carbon chain propagation via alkyl coupling.[2−4] Most metal surfaces preferentially dehydrogenate adsorbed alkyls and thus are not suitable for studying carbon−carbon bond formation. Exceptions include the coinage metals: the relative inertness of copper, silver, and gold allows adsorbed alkyls to selectively undergo the coupling reaction.

Methylene (CH_2) insertion into metal−carbon bonds has long been postulated as a Fischer−Tropsch chain growth step,[5] but no direct spectroscopic evidence has been offered. The difficulty lies in isolating and characterizing the transient intermediates. Thus, temperature-programmed reaction spectroscopy (TPRS) has been employed to identify the final gas-phase products from which the mechanism and kinetics have been indirectly deduced. Indirect evidence comes mainly from the reaction of adsorbed methylene (CH_2(a)) on Cu,[6−8] Ag,[9−11] and oxygen-modified Mo[12] surfaces, where the final gas-phase products included higher hydrocarbons. However, as Zheng et al. pointed out,[13] the coupling of alkyl fragments on metal surfaces to form carbon−carbon bonds consists of several elementary steps: chemisorption, migration, organization of fragments prior to reaction, and, finally, actual coupling and desorption. The rate-controlling step has not been identified unambiguously. Moreover, when alkyl iodides are used to generate alkyl groups, we must also consider the rupture of the carbon−halogen bond, a feature depending on both the metal surface and the alkyl halide,[14,15] and the coexistence of iodine on the surface. The TPRS technique cannot distinguish among the effects of these various steps on the coupling reaction. Therefore, for a thorough understanding of Fischer−Tropsch synthesis, it is both important and challenging to find information that relates directly to the CH_2 insertion step.

Recently, Wu et al. employed TPRS to study carbon−carbon bond formation by CH_2 insertion into adsorbed methyl (CH_3-(a)) and adsorbed perfluoromethyl (CF_3(a)) on Ag(111).[9,10] With

† Current address: Fritz-Haber-Institut der Max-Planck-Gesellschaft, Berlin 14195, Germany.

(1) Anderson, R. B. *The Fischer−Tropsch Synthesis*; Academic Press: New York, 1984.
(2) Zhou, X. L.; Zhu, X. Y.; White, J. M. *Surf. Sci. Rep.* **1991**, *13*, 73−220.
(3) Zaera, F. *Chem. Rev.* **1995**, *95*, 2651−2693.
(4) Bent, B. E. *Chem. Rev.* **1996**, *96*, 1361−1390.
(5) Brady, R. C., III; Pettit, R. *J. Am. Chem. Soc.* **1980**, *102*, 6181−6182.
(6) Chiang, C. M.; Wentzlaff, T. H.; Bent, B. E. *J. Phys. Chem.* **1992**, *96*, 1836−1848.
(7) Lin, J. L.; Chiang, C. M.; Jenks, C. J.; Yang, M. X.; Wentzlaff, T. H.; Bent, B. E. *J. Catal.* **1994**, *147*, 250−263.
(8) Chuang, P.; Chan, Y. L.; Chien, S. H.; Klauser, R.; Chuang, T. J. *Chem. Phys. Lett.* **2002**, *354*, 179−185.
(9) Wu, H. J.; Chiang, C. M. *J. Phys. Chem. B* **1998**, *102*, 7075−7077.
(10) Wu, H. J.; Hsu, H. K.; Chiang, C. M. *J. Am. Chem. Soc.* **1999**, *121*, 4433−4442.
(11) Scheer, K. C.; Kis, A.; Kiss, J.; White, J. M. *Top. Catal.* **2002**, *20*, 43−51.
(12) Kim, S. H.; Stair, P. C. *J. Am. Chem. Soc.* **1998**, *120*, 8535−8536; *J. Phys. Chem. B* **2000**, *104*, 3035−3043.
(13) Zheng, C.; Apeloig, Y.; Hoffmann, R. *J. Am. Chem. Soc.* **1988**, *110*, 749−774.
(14) Buelow, M. T.; Zhou, G.; Gellman, A. J.; Immaraporn, B. *Catal. Lett.* **1999**, *59*, 9−13.
(15) Buelow, M. T.; Gellman, A. J. *J. Am. Chem. Soc.* **2001**, *123*, 1440−1448.

CF_3(a) as the target for CH_2 insertion, a desorption signal for CF_2═CH_2 was detected, and CF_3CH_2(a) formed via CH_2 insertion was proposed as the reaction intermediate. Because CF_3CH_2(a) is thermally stable up to ~200 K, where the β-fluorine elimination reaction occurs on Ag(111),[16] the CH_2 insertion reaction can be distinguished from the subsequent CF_3-CH_2(a) elimination reaction provided insertion occurs below 200 K. This opens the possibility of directly studying the CH_2 insertion reaction. Consequently, we combined RAIRS and TPRS to investigate the cross coupling between CH_2(a) and CF_3-(a). In our previous communication,[17] CF_3CH_2(a) was spectroscopically unequivocally identified as the product of the CH_2 insertion reaction; herein, we report detailed spectroscopic results concerning the mechanism and kinetics of this reaction. Sequential CH_2 insertion into Ag−CF_3 occurs provided the coverages of reactants are high, as evidenced by $CH_2CH_2CF_3$-(a) formation detected with RAIRS. It is noteworthy that the high IR-sensitivity of CF_3CH_2(a) enables us, for the first time, to directly investigate the insertion reaction kinetics using time-resolved RAIRS (TR-RAIRS). Our results reveal important new insights into the methylene insertion reaction not available in previous TPRS studies.

2. Experimental Section

We conducted our experiments in a two-level stainless steel ultrahigh-vacuum (UHV) chamber.[18] The upper level is equipped with a Nicolet Magna-IR 860 spectrometer for RAIRS, a SRS RGA 200 for residual gas analysis (RGA), and an ion sputtering gun; the lower level is comprised of a UTI-100C mass analyzer for TPRS, and a single-pass cylindrical mirror analyzer for Auger electron spectroscopy (AES). Turbo-molecular pumps brought the chamber to a base pressure of $(1.0-2.0) \times 10^{-10}$ Torr.

The Ag(111) sample was mounted on a tungsten loop attached to rectangular cross-section copper bars that were electrically isolated from a hollow copper block filled with liquid nitrogen. Resistive heating of the sample was accomplished through a high current power supply connected to the tungsten loop. Sample temperatures between 80 and 1000 K were obtained using a commercial temperature controller, and the surface temperature was measured with a type K thermocouple inserted into a hole at the crystal's edge.

The Ag(111) surface was initially cleaned by repeated cycles of Ar^+ sputtering and annealing, until no contaminants were detected in AES. After each experiment, the surface was cleaned again by heating to 960 K, to desorb atomic iodine and AgF.[10] Diiodomethane (CH_2I_2, 99% purity, Aldrich) and 2,2,2-trifluoroethyl iodide (CF_3CH_2I, 99% purity, Lancaster) were used as received except that we removed dissolved gases by several cycles of freeze−pump−thaw prior to experiments. The gaseous compound trifluoromethyl iodide (CF_3I, 99% purity, Aldrich) was used as received. All purities were verified by RGA.

A preset leak valve ending in a capillary-array was used to dose adsorbates. During dosing, the doser tube ended 2 mm in front of the sample; after dosing, it was retracted 25 mm. A fixed pressure of adsorbate was added to a vessel behind a closed butterfly valve connected by an evacuated tube to the leak valve. The leak valve was preset to obtain a chamber pressure rise of 3.0×10^{-10} Torr when all surfaces in the chamber were at 300 K. With the substrate cooled to the desired temperature, the butterfly valve was opened to initiate the dose. The dose was terminated by evacuating the gas behind the leak valve with a turbo-molecular pump rather than closing the leak valve, a procedure that yielded excellent experimental reproducibility (±2%) of TPD spectra. Because careful calibration by comparing the integrated areas of CF_3 radical desorption peaks at a given exposure indicates that the surface exposure is 30× that obtained by backfilling the chamber, we have multiplied by 30 to get the exposures in Langmuir (1 L = 1.0×10^{-6} Torr s), that is, exposure in L = $30 \times 3 \times 10^{-4} \times t$, where t is the dose time (s).

TPRS spectra were collected at a ramp rate of 1 K s^{-1}, with a maximum of eight different *m*/*e* values recorded for each experiment. RAIRS spectra were collected, using a mercury−cadmium telluride (MCT) detector, by co-adding 1500 scans at 4 cm^{-1} resolution (data capture lasting about 15 min); RAIRS for clean Ag(111) served as the reference. The fast scan function of the IR spectrometer allowed for time-resolved RAIRS (TR-RAIRS). Each spectrum was collected by co-adding 20 fast scans at 4 cm^{-1} resolution, which gives a temporal resolution of 1.8 s. To gather TR-RAIRS data, we first exposed the Ag(111) surface to 0.5 L CF_3I; continuous capture of RAIRS spectra then began a few seconds before dosing 0.2 L CH_2I_2 (dosing time = 23 s). Data capture for TR-RAIRS lasted about 5 min.

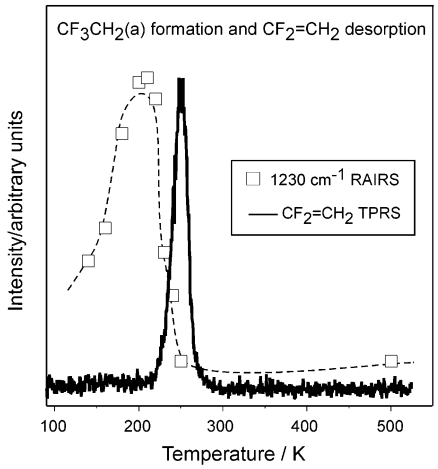

Figure 1. Comparison between the temperature-dependent formation and loss of CF_3CH_2(a) (represented by the 1230 cm^{-1} RAIRS peak intensity) and the desorption trace (intensity multiplied by 0.1) of CF_2═CH_2 following a 0.2 L CH_2I_2/0.5 L CF_3I dose at 90 K on Ag(111). The corresponding TPRS and RAIRS spectra have been reported in ref 17.

3. Results

Low Coverages: CH_2(a) Insertion into Ag−CF_3(a). The main experimental results of this part have been reported in our previous communication.[17] Here, we only give a brief summary. Coadsorption of 0.2 L CH_2I_2 after 0.5 L CF_3I (denoted 0.2 L CH_2I_2/0.5 L CF_3I) at 90 K gives rise to a desorption peak of CF_2═CH_2 at 250 K in the TPRS spectra. The RAIRS spectra after a 0.2 L CH_2I_2/0.5 L CF_3I dose at 90 K followed by annealing confirm the formation of CF_3CH_2(a) at elevated temperatures on the surface. Figure 1 compares the evolution of CF_3CH_2(a) (represented by the vibrational feature at 1230 cm^{-1} in the RAIRS spectrum at various annealing temperatures) with the desorption trace of CF_2═CH_2. CF_3CH_2(a) forms between 140 and 210 K, and then undergoes reaction. The reaction of CF_3CH_2(a) on Ag(111) exactly coincides with the desorption of CF_2═CH_2. These experimental results provide a clear reaction scheme: migratory CH_2(a) inserts into Ag−CF_3(a), producing CF_3CH_2(a) that undergoes β-fluoride elimination to form CF_2═CH_2.[17]

High Coverages: Sequential Insertion of CH_2(a). New desorption features arise with increasing exposure of CH_2I_2 or CF_3I (Figure 2). For a 0.2 L CH_2I_2/0.5 L CF_3I dose, there is a single 64 amu peak at 250 K, attributed to CF_2═CH_2 desorption. Increasing the CF_3I dose to 0.9 L results in the emergence of a

(16) Paul, A.; Gellman, A. J. *Langmuir* **1995**, *11*, 4433−4439.
(17) Huang, W. X.; White, J. M. *J. Am. Chem. Soc.* **2003**, *125*, 10798−10799.
(18) Huang, W. X.; White, J. M. *Surf. Sci.* **2002**, *513*, 399−404.

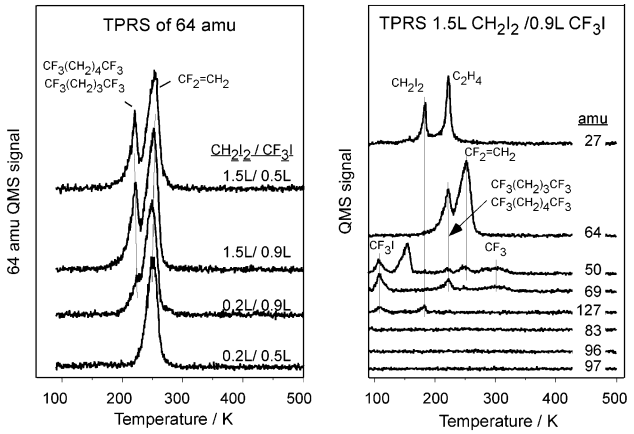

Figure 2. TPRS profiles for $C_2F_2H_2^+$ following indicated doses of CF_3I and CH_2I_2 (left panel), and selected ions for a 1.5 L CH_2I_2/0.9 L CF_3I dose at 90 K (right panel).

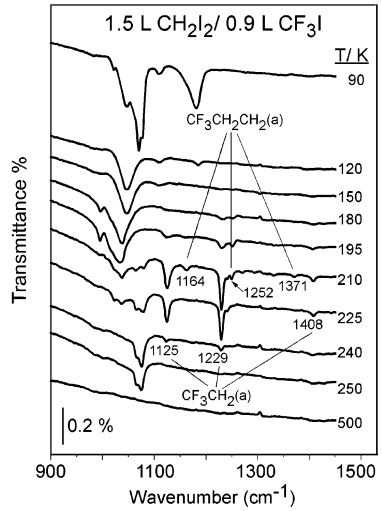

Figure 3. RAIRS for a 1.5 L CH_2I_2/0.9 L CF_3I dose on Ag(111) at 90 K, followed by annealing at indicated temperatures for 2 min. Spectra were recorded at 90 K.

shoulder at 226 K. The peak grows when the CH_2I_2 coverage is increased to 1.5 L. The right panel of Figure 2 shows several ion profiles after a 1.5 L CH_2I_2/0.9 L CF_3I exposure. The 226 K peak has a fragmentation pattern different from that of CF_2=CH_2; there is a 69 amu fragment that does not appear at 250 K. The peaks at 300, 222, 183, and 107 K are assigned to CF_3, C_2H_4, CH_2I_2, and CF_3I desorption, respectively. The peak at 107 K is ascribed to multilayer CF_3I desorption.

Before we discuss the likely new product on the basis of the fragmentation pattern, we first examine RAIRS (Figure 3) after a 1.5 L CH_2I_2/0.9 L CF_3I dose followed by annealing. At 90 K, there is a peak at 1182 cm^{-1} and a complex multipeak structure around 1070 cm^{-1}, assigned to both monolayer and multilayer CF_3I(a). Annealing at 120 K desorbs the multilayer and breaks the C−I bond of monolayer CF_3I(a), thus forming the single peak at 1046 cm^{-1}. Changes are not evident after annealing to 150 K, but annealing at 180 K produces several new vibrational bands that can be divided into two groups on the basis of their intensity changes. One group includes the peaks at 1125, 1229, and 1408 cm^{-1}, which, according to previous results,[17] can be assigned to CF_3CH_2(a) formed via CH_2(a) insertion into Ag−CF_3. The other group includes the peaks at 1164, 1252, and 1371 cm^{-1}, which grow between 180 and 210 K and disappear after 225 K. By comparison with the vibrational spectrum of $CF_3CH_2CH_2$(a) prepared by thermal dissociation of CF_3CH_2-CH_2I on Cu(111),[20] we assign the latter three peaks to the C−F symmetric stretch, CH_2 deformation, and CH_2 twist of CF_3CH_2-CH_2(a) on Ag(111), respectively (Table 1). These spectroscopic results reflect multiple insertion of CH_2(a) into Ag−CF_3 provided there are sufficient CH_2(a) and CF_3(a). Furthermore, the bands assigned to CF_3CH_2(a) and $CF_3CH_2CH_2$(a) appear to intensify together between 180 and 210 K, indicating the paths leading to both species are readily accessible.

Table 1. Assignment of Vibrations: CF_3CH_2(a) and $CF_3CH_2CH_2$(a) on Ag(111)

	CF_3CH_2(a) on Ag(111)	CF_3CH_2I (l) (from ref 19)	$CF_3CH_2CH_2$(a) on Ag(111)	$CF_3CH_2CH_2$(a) on Cu(111) (from ref 20)
CF stretch	1004	1049		
CF stretch	1114	1114	1164	1170
CH_2 deformation	1227	1257	1252	1265
CH_2 twist			1371	1350
CF stretch	1409	1423		

Because the disappearance of vibrational bands assigned to $CF_3CH_2CH_2$(a) coincides with desorption of the new product, we infer that the new product comes from a reaction of CF_3-CH_2CH_2(a). When generated by thermal dissociation of CF_3-CH_2CH_2I, $CF_3CH_2CH_2$(a) mainly self-couples to produce $CF_3(CH_2)_4CF_3$, with only a minor contribution from β-hydrogen elimination to produce CF_3CH=CH_2.[21] Furthermore, the recombination of $CF_3CH_2CH_2$(a) with I(a) to produce CF_3CH_2-CH_2I has been reported when the I(a) coverage is very high.[10] The absence of peaks for CF_3CH=CH_2^+ (96 amu), CF_3CH_2-CH_2^+ (97 amu), and I^+ (127 amu) indicates that, under our experimental conditions, alkyl iodide is not formed; rather CF_3-CH_2CH_2(a) either self-couples or cross-couples with CF_3CH_2-(a) to produce either $CF_3(CH_2)_4CF_3$ or $CF_3(CH_2)_3CF_3$. Fragmentation of these accounts for the $CF_2CH_2^+$, CF_3^+, and CF_2^+ peaks. Making the assignment of the desorption species somewhat uncertain, the standard fragmentation patterns for $CF_3(CH_2)_4CF_3$ and $CF_3(CH_2)_3CF_3$ were not available. However, sequential insertion of CH_2(a) into Ag−CF_3 to form CF_3CH_2-CH_2(a) is unambiguous on the basis of RAIRS.

TR-RAIRS: Kinetics of the Insertion Reaction. We found that the insertion reaction is discernible at 140 K when the surface, exposed to a 0.2 L CH_2I_2/0.5 L CF_3I dose at 90 K, is annealed.[17] When dosing occurs at higher temperatures, the reaction is evident as low as 120 K (Figure 4). These findings imply that the migratory insertion of CH_2(a) into Ag−CF_3(a) is very facile on Ag(111).

Because of the high IR-sensitivity of the vibrational features of CF_3CH_2(a), the kinetics of the methylene insertion could be followed above 120 K by TR-RAIRS. For these temperatures, CF_3(a) and CH_2(a) are produced by a dose of 0.2 L CH_2I_2/0.5 L CF_3I, leaving no C−I bonds to be accounted for in the kinetics. The left panel of Figure 5 displays a typical series of TR-RAIRS spectra following dosing at 180 K. The starting surface (lowest curve) is precovered by CF_3(a), showing a

(19) Harnish, D. F.; Hirschmann, R. P. *Appl. Spectrosc.* **1970**, *24*, 28−35.
(20) Forbes, J. G.; Gellman, A. J. *J. Am. Chem. Soc.* **1993**, *115*, 6277−6283.
(21) Paul, A.; Gellmann, A. J. *J. Am. Chem. Soc.* **1995**, *117*, 9056−9066.

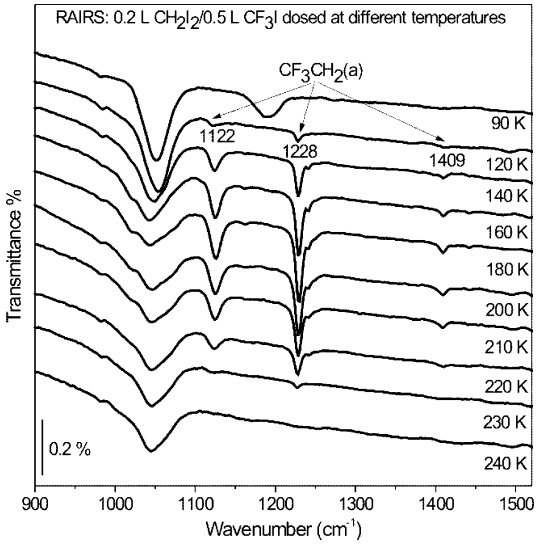

Figure 4. RAIRS spectra following a 0.2 L CH_2I_2/0.5 L CF_3I dose onto Ag(111) at different temperatures. The formation of CF_3CH_2(a) is evident at a temperature as low as 120 K.

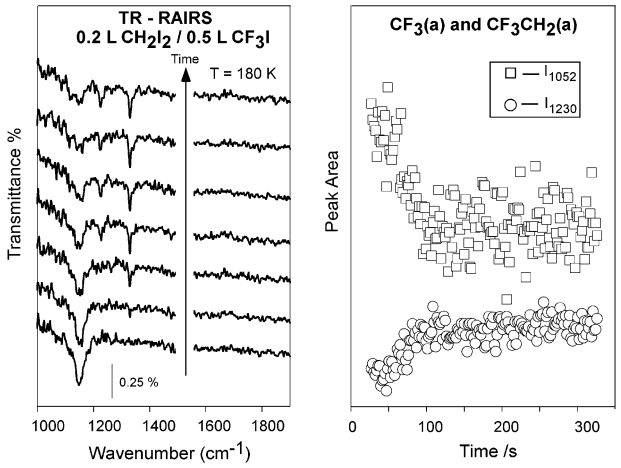

Figure 5. Left panel: Time-resolved RAIRS following a 0.2 L CH_2I_2/0.5 L CF_3I dose on Ag(111) at 180 K. Right panel: Temporal evolutions of CF_3(a) (represented by the peak at 1052 cm^{-1}) and CF_3CH_2(a) (represented by the peak at 1230 cm^{-1}) during the course of the insertion reaction.

vibrational peak only at 1052 cm^{-1}. When CH_2(a) is introduced, the surface reaction commences and two vibrational bands (1126 and 1230 cm^{-1}) grow at the expense of the 1052 cm^{-1} band. Integrating the areas of the peaks at 1052 (representing CF_3(a)) and 1230 cm^{-1} (representing CF_3CH_2(a)) at 1.8 s intervals gives the right panel of Figure 5. Clearly, reaction of CF_3(a) with CH_2(a) leads to CF_3CH_2(a).

The slopes of the curves in the right panel of Figure 5 reflect the consumption rate of CF_3(a) and the formation rate of CF_3CH_2(a). Because CF_3CH_2(a) has a vibrational peak at 1020 cm^{-1} that contributes to the integrated area of the 1050 cm^{-1} CF_3(a) band, the 1230 cm^{-1} CF_3CH_2(a) band was used to quantitate the insertion reaction kinetics. Between 140 and 180 K, the rate increases (Figure 6), but when the reaction temperature exceeds 200 K, β-fluorine elimination sets in and the 1230 cm^{-1} time dependence monitors both production and consumption of CF_3CH_2(a). Considering both the insertion reaction and the β-fluorine elimination reaction, the rate equation describing CF_3CH_2(a) can be written in terms of the insertion rate r_i and the elimination rate, r_e:

$$\frac{d[CF_3CH_2]_a}{dt} = r_i - r_e = k_i[CH_2]_a[CF_3]_a - k_e[CF_3CH_2]_a$$

To determine at which temperature the elimination reaction is detectable, we dosed 0.2 L CF_3CH_2I on Ag(111) at different temperatures. The RAIRS results clearly show that CF_3CH_2(a) undergoes defluorination above 180 K (Figure 7). Thus, for $T \leq 180$ K,

$$\frac{d[CF_3CH_2]_a}{dt} = k_i[CH_2]_a[CF_3]_a$$

Assuming a proportional relationship between the integrated area of the RAIRS peak and the coverage of the surface species up to monolayer coverage,[22] an Arrhenius plot for $T \leq 180$ K (inset

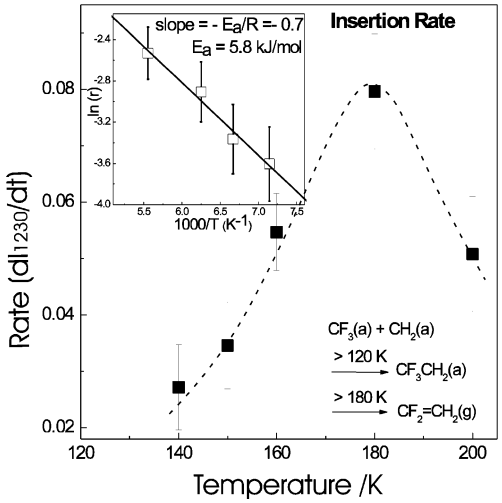

Figure 6. Reaction rates of the insertion reaction of CH_2(a) into Ag−CF_3 at various reaction temperatures, determined by TR-RAIRS at various temperatures (right panel of Figure 5). Inset: Arrhenius plot of rate data.

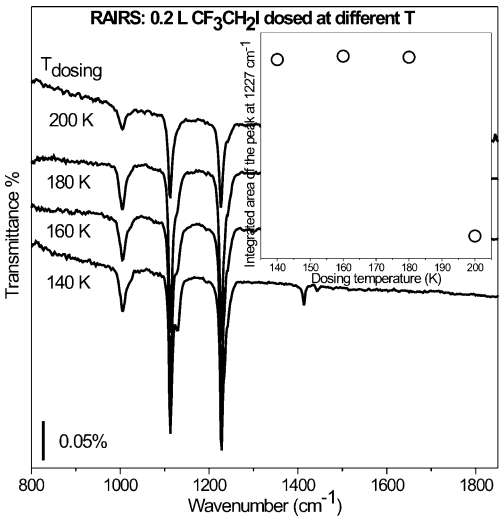

Figure 7. RAIRS spectra following a 0.2 L CF_3CH_2I dose onto Ag(111) at different temperatures. The inset shows the surface coverages of CF_3CH_2(a) (represented by the peak area of 1227 cm^{-1}) produced by a 0.2 L CF_3CH_2I dose at different substrate temperatures, demonstrating that CF_3CH_2(a) undergoes defluorination reaction above 180 K.

(22) Persson, B. N. J. *Solid State Commun.* **1979**, *30*, 163−166.

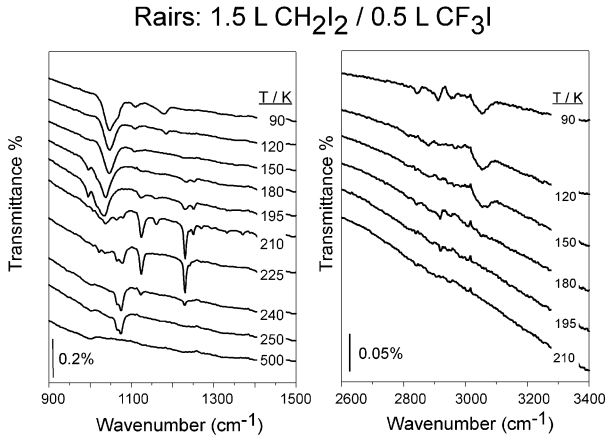

Figure 8. RAIRS of a 1.5 L CH_2I_2/0.5 L CF_3I dose at 90 K, followed by annealing at indicated temperatures for 2 min. Spectra were recorded at 90 K.

to Figure 6) gives a very low activation energy (5.8 kJ mol^{-1}) for methylene insertion into Ag−CF_3(a) on Ag(111). This low activation energy is consistent with our observation that the insertion reaction occurs even at 120 K.

4. Discussion

Insertion of CH_2(a) into Ag−CF_3: Mechanism. Although several studies have reported the overall chain propagation reaction via CH_2(a) insertion, our results give, for the first time, direct evidence of events on the surface. Using CF_3(a) instead of CH_3(a) as the target must be considered, but the evidence indicates that CH_2(a) insertion into CH_3(a) is also facile on Ag(111). It has been reported that on Ag(111) the fluorine substitution increases the activation energy for the coupling reaction of alkyls[21] and decreases the activation energy of C−I bond rupture.[15]

Spectroscopic results provide clear evidence for CF_3CH_2(a) and $CF_3CH_2CH_2$(a) formation via the CH_2 insertion reaction. The insertion reaction occurs at 120 K following a 0.2 L CH_2I_2/0.5 L CF_3I dose. Higher temperatures are required for the occurrence of the insertion reaction when the CF_3 coverage is higher, for example, for a 1.5 L CH_2I_2/0.9 L CF_3I dose. The difference comes from the coverage-dependent C−I rupture; as revealed by RAIRS, the first case produces CH_2(a), while the latter produces CH_2I_2(a). Figure 8 displays the RAIRS spectra following a 1.5 L CH_2I_2/0.5 L CF_3I dose. At 90 K, both adsorb molecularly. The vibrational band at 3053 cm^{-1} corresponds to the CH_2 asymmetric stretch of CH_2I_2(a).[11] The C−I bonds of CF_3I(a) rupture after annealing at 120 K, but those of CH_2I_2(a) require annealing to 180 K. Coincidentally, CF_3CH_2(a) and $CF_3CH_2CH_2$(a) formation becomes obvious after annealing at 180 K. This consistency clearly demonstrates that CF_3CH_2(a) and $CF_3CH_2CH_2$(a) come from the insertion of CH_2(a) into Ag−CF_3.

Previous TPRS results have established first-order kinetics for the bimolecular alkyl coupling reaction on coinage metal surfaces. That first, not second, order kinetics were observed was attributed to islanding of the alkyl fragments prior to the coupling reaction. We note that CF_3CH_2(a) and $CF_3CH_2CH_2$-(a) form simultaneously on Ag(111) (Figures 3 and 8), and this is also consistent with assembly of the alkyl fragments (CH_2(a) and CF_3(a)) into islands prior to the occurrence of the insertion reaction. In this situation, time-consuming diffusion steps are not needed to accomplish the chain propagation. Fragment islanding is also consistent with complicated changes in the C−F stretch vibrations that occur between 1000 and 1100 cm^{-1} during the course of the insertion reaction. When reaction-involved fragments reside as neighbors within an island, the reaction can alter the local environments. First-order kinetics, as for coupling reaction of alkyls, would be expected for such an island model.

Insertion of CH_2(a) into Ag−CF_3: Kinetics. The activation barrier, 5.8 kJ/mol, for CH_2 insertion into Ag−CF_3(a) is lower than expected. Reported barriers for the coupling reaction of various alkyls are between 60 and 80 kJ/mol on Ag(111).[21] The barrier for CH_2(a) insertion into Cu−CD_3(a) was reported to be 60 and 80 kJ/mol on Cu(100) and Cu(110).[6,7] These previously reported kinetic parameters for the coupling of alkyl groups on single metal surfaces are all indirectly determined from TPRS studies, which must assume that product desorption is reaction-limited and that alkyl group generation via C−I rupture does not affect the coupling reaction. While the first assumption is satisfied on the basis of TPD spectra of the directly adsorbed product molecules from the same surface, the second has not been scrutinized. The C−I bonds of alkyl iodides are usually thermally broken below 200 K; thus, if the reaction of the alkyl group occurs far above 200 K, it will not be affected by the C−I rupture. On the other hand, if alkyl reaction occurs below 200 K, C−I rupture could have an impact. The self-coupling of CH_2(a) on Cu(100) provides a good example: evolution of C_2H_4 occurs at 180 K provided that CH_2(a) is formed upon adsorption, but occurs at 230 K if CH_2I_2(a) is adsorbed.[7]

The self-coupling[11] and the insertion reaction of CH_2(a) reported here on Ag(111) also illustrate the critical point that, to abstract the true kinetic parameters of the alkyl coupling reaction from TPRS results, one must be certain that the starting surface is covered by the alkyl fragments, not by molecular adsorbates. Our RAIRS results confirm the formation of CH_2-(a) and CF_3(a) following a 0.2 L CH_2I_2/0.5 L CF_3I dose above 120 K. In this respect, the activation energy for the insertion reaction derived from TR-RAIRS results is reliable. Although the activation barrier of CH_2(a) insertion into Ag−CF_3(a) is extremely low, there is both experimental[23] and theoretical[24] evidence that carbene inserts into H−H and C−H bonds with no energy barrier.

Although TPRS is not controlled by the formation of CH_2-CF_3(a), it is interesting to use the RAIRS data to predict what TPRS would give for an activation energy were desorption controlled by this formation reaction. On the basis of the RAIRS data (Figure 1), the maximum desorption rate for CF_2═CH_2 would be expected to be at or below 210 K in TPRS. Assuming a rate maximum between 140 and 210 K and a pseudo first-order pre-exponential factor of 10^{13} s^{-1}, Redhead analysis[25] yields an activation energy for CH_2(a) insertion into Ag−CF_3-(a) of 34−39 kJ/mol (assuming a maximum rate at 140 K) and 50−60 kJ/mol (assuming a maximum rate at 210 K) as the heating rate varies from 10 to 0.1 K/s. Although aligning reasonably well with some previous estimates for insertion reactions,[7] this rough analysis predicts an activation energy that is nearly an order of magnitude higher than that obtained by

(23) Kirmse, W. *Carbene Chemistry*; Academic Press: New York, 1971.
(24) Kollmar, H. *J. Am. Chem. Soc.* **1978**, *100*, 2660−2664.
(25) Redhead, P. A. *Vacuum* **1962**, *12*, 203−211.

monitoring the temperature dependence of the RAIRS data. In our judgment, the activation energy determined from the RAIRS data (5.8 kJ/mol) gives a much more dependable picture of the facile insertion of CH_2 into $Ag-CF_3$. TR-RAIRS provides the average isothermal reaction rates at different reaction temperatures, starting with the same coverages, whereas TPRS reflects the transient desorption rate at various temperatures and different instantaneous coverages of reactants.

Comparison with Other Work. The self-coupling of alkyl fragments and the CH_2 insertion reaction have been observed mainly on coinage metals. The reaction rate of CH_3(a) was systematically compared on several Cu, Ag, and Au single-crystal surfaces; CH_3(a) self-couples fastest on Ag(111).[26] This was attributed to both the weakest metal−carbon bond for CH_3-(a) on Ag(111) and the lowest Fermi level of Ag(111).[26] Similarly, the CH_2(a) self-coupling reaction and the CH_2(a) + CH_3(a) reaction occurs with a lower barrier on Ag(111) than on Cu(100) or Cu(111). Via CH_2(a) self-coupling, C_2H_4 evolves at 142 K on Ag(111),[17] 220 K on Cu(100),[7] and 300 K on Cu(110).[7] The desorption of CH_2CD_2 controlled by CH_2(a) and CD_3(a) appears, respectively, at 260 and 315 K on Cu(100) and Cu(110).[7] Figure 1 implies that the maximum CH_2CF_3(a) formation rate occurs around 210 K. These results suggest that silver is a good catalyst for the low-temperature chain propagation reaction via methylene insertion, provided alkyl fragments form on the surface. A recent theoretical calculation for CH_x reactions on Ru predicts that CH_2(a) is kinetically unstable due to the extremely low barrier to decomposition into stable CH-(a) and that insertion of CH_2(a) into CH_3(a) has the highest barrier for insertion among the studied reaction routes.[27] However, on Ag(111), because of its inertness in cleaving C−H bonds, CH_2(a) is stable and can facilely insert into the Ag−CF_3(a).

5. Conclusions

We have successfully clarified the mechanism and kinetics of the insertion reaction of methylene into $Ag-CF_3$(a) by means of reflection−absorption infrared spectroscopy (RAIRS) on Ag(111). CF_3CH_2(a) and $CF_3CH_2CH_2$(a), respectively, were spectroscopically identified as the intermediates of the insertion and sequential insertion of CH_2(a) into $Ag-CF_3$(a). The insertion reaction barrier was 5.8 kJ/mol, determined using time-resolved reflection−absorption infrared spectroscopy. These results provide, for the first time, direct spectroscopic information on the methylene insertion reaction.

Acknowledgment. This work was supported by the U.S. Department of Energy's Chemical Sciences, Geosciences, and Biosciences Division/Office of Basic Energy Sciences, and by the Robert A. Welch Foundation, Grant F-0032.

JA047423B

(26) Paul, A.; Bent, B. E. *J. Catal.* **1994**, *147*, 264−271.

(27) Liu, Z. P.; Hu, P. *J. Am. Chem. Soc.* **2002**, *124*, 11568−11569.